Extraction of Hydrographic Regions from Remote Sensing Images Using an Oscillator Network with Weight Adaptation

Xiuwen Liu, Ke Chen, and DeLiang Wang

***Abstract*—We propose a framework for object extraction with accurate boundaries. A multilayer perceptron is used to identify seed points through examples, and regions are extracted and localized using a locally coupled network with weight adaptation. A functional system has been developed and applied to hydrographic region extraction from Digital Orthophoto Quarter–Quadrangle images.**

***Index Terms*—Classification, hydrographic region extraction, LEGION, multilayer perceptron, weight adaptation.**

I. Introduction

With the availability of remotely sensed high resolution imagery and advances in computing technologies, cost-effective and efficient ways to generate accurate geographic information are possible. However, geographic information is encoded implicitly in images, and a critical step is to extract geographic information and make it explicit. For remote sensing applications, classification is one of the most commonly used techniques to extract quantitative information from images, and multilayer perceptrons have been widely used due to their learning capability through examples [3], [12], [1], [10]. For classification approaches, there is an intrinsic tradeoff between regional and boundary accuracy. When a large window is used, the classification result within a homogeneous region tends to be accurate but with a large boundary uncertainty. For a small window, the boundaries tend to be accurate. However, the classification result can be very noisy even within a homogeneous region.

We attempt to develop a framework for automated feature extraction that can derive accurate geographic information. In this communication, we pose the automated feature extraction problem as a binding problem. Pixels that belong to desired regions should be bound together to form meaningful objects. We use a locally excitatory globally inhibitory oscillator networks (LEGION) network [11], [14], [15], which provides a generic framework for feature binding and image segmentation. As shown analytically [11], LEGION networks can achieve both synchronization within an oscillator group representing a region and desynchronization among different oscillator groups rapidly. This offers a theoretical advantage over pure local networks such as Markov Random Fields, where efficient convergence has not been established. To improve the performance, we incorporate contextual information through a weight adaptation method proposed by Chen *et al.* [2]. The weight adaptation method can be viewed as a way of incorporating contextual information by relating detected structures at two different scales. In weight adaptation, statistical information from a larger scale is derived and mainly used to govern a locally coupled adaptation process, resulting in accurate boundary localization and robustness to noise. We assume that features to be extracted are specified through examples, and we use a multilayer perceptron to determine regions with significant features. This training methodology greatly reduces the number of necessary training samples. We have developed a functioning system using the proposed method for hydrographic feature extraction from digital orthophoto quarter–quadrangle (DOQQ) images and have obtained satisfactory results.

Manuscript received April 13, 1999; revised December 16, 1999. This work was partially supported by the Center for Mapping, The Ohio State University, Columbus, the National Imagery, NSF Grant (IRI-9423312), and the ONR Young Investigator Award (N00014-96-1-0676).

X. Liu is with the Department of Computer Science, Florida State University, Tallahassee, FL 32306 USA (e-mail: liux@cs.fsu.edu).

K. Chen was with the Center for Cognitive Science and the Department of Computer and Information Science, The Ohio State University, Columbus, OH 43210 USA. He is now with the National Laboratory of Machine Perception and Center for Information Science, Peking University, Beijing 100871, China (e-mail: chen@cis.pku.edu.cn).

D. Wang is with the Center for Cognitive Science and the Department of Computer and Information Science, The Ohio State University, Columbus, OH 43210 USA (e-mail: dwang@cis.ohio-state.edu).

Publisher Item Identifier S 0196-2892(01)00475-2.

II. Methodology

Through theoretical investigation of brain functions, von der Malsburg [13] hypothesized that temporal correlation provides a generic framework for feature binding, and Terman and Wang proposed LEGION networks [11], [14], [15] as a computational framework for feature binding and image segmentation. In LEGION networks, an object is represented by a group of synchronized oscillators, and different objects are represented by groups that are desynchronized. It has been shown analytically that LEGION networks can rapidly achieve both synchronization in a locally coupled oscillator group and desynchronization among different oscillator groups [11], [14], [15]. LEGION has been successfully applied to segmenting gray level images [14], [15], range images [5], and medical images [8].

A. Single Oscillator

As the building block of a LEGION network, a single oscillator is defined as a feedback loop between an excitatory unit x and an inhibitor unit y [11], [14], [15]

$$\frac{dx}{dt} = 3x - x^3 + 2 - y + IH(p-\theta) + S + \rho \tag{1a}$$

$$\frac{dy}{dt} = \epsilon(\alpha(1+\tanh(x/\beta)) - y). \tag{1b}$$

Here, H is the Heaviside step function, I represents external stimulation to the oscillator, and S represents overall coupling from other oscillators in the network. The *potential* associated with the oscillator p is introduced to distinguish fragments from major regions [14], [15], and θ is a threshold. Basically, only oscillators within a large homogeneous region can develop a potential larger than threshold θ and thus receive effective external stimuli. These oscillators are referred to as *leaders*. Oscillators that belong to noisy regions cannot develop high potentials and are suppressed into a background region. See Wang and Terman [14], [15] for more details regarding the potential term. The parameter ρ denotes a Gaussian noise term and is introduced to test the robustness of the system and to facilitate desynchronizing different input patterns.

The parameter ϵ is chosen to be a small positive number, i.e., $0 < \epsilon \ll 1$. Under this condition, without any coupling S or noise ρ, (1) corresponds to a standard relaxation oscillator. For a positive external stimulus, i.e., $I > 0$, (1) has a stable periodic solution for all sufficiently small ϵ. The periodic solution alternates between the *active phase* and the *silent phase*. Within these two phases, (1) exhibits near steady state behavior and the oscillator travels on a slow time scale. In contrast, the transition between two phases occurs on a fast time scale. The highly nonlinear behavior leads to desirable properties for binding and segmentation. For $I < 0$, (1) has a stable fixed point. In this case, the oscillator needs to receive excitatory coupling from other oscillators in order to oscillate.

B. LEGION for Image Segmentation

A LEGION network for image segmentation consists of locally coupled relaxation oscillators and a global inhibitor. In the two-dimensional case, an oscillator is denoted by (i, j), where i and j indicate the row and column of the oscillator. In LEGION, the coupling term S_{ij} for oscillator (i, j) in (1) is given by [2]:

$$S_{ij} = \frac{\sum_{(k,l)\in N(i,j)} H(x_{kl})/(1+|W_{ij;kl}|)}{\log\left(\sum_{(k,l)\in N(i,j)} H(x_{kl})+1\right)} - W_z H(z-\theta_z) \quad (2)$$

where the first term is total excitatory coupling that oscillator (i, j) receives from the oscillators in a local neighborhood $N(i, j)$. $W_{ij;kl}$ is the dynamic connection from oscillator (k, l) to (i, j), and it encodes dissimilarity to simplify the equations for weight adaptation, hence the reciprocal[1] in (2). Note that, unlike in [14], [15], the first term in (2) implements a logarithmic grouping rule [2], which generates better segmentation results. In the second term, θ_z is a threshold, and the global inhibitor z is defined as $dz/dt = \phi(\sigma_\infty - z)$, where $\sigma_\infty = 1$ if $x_{ij} \geq \theta_z$ for at least one oscillator (i, j) in the entire network, and $\sigma_\infty = 0$ otherwise. The parameter ϕ determines the rate at which the global inhibitor reacts to such stimulation. If the activity of at least one oscillator is above θ_z, the global inhibitor approaches to 1, and in turn it sends inhibition to the entire network. W_z in (2) is the weight of inhibition from the global inhibitor. This leads to desynchronization among different oscillator groups [11], [14], [15].

The computation of LEGION can be summarized as follows. An oscillator triggers the global inhibitor when it jumps to the active phase. As a result, the global inhibitor is activated and exerts inhibition on all oscillators in the network. On the other hand, an oscillator in the active phase propagates its activation to its local neighbors through the local coupling as shown in the first term of (2), and the excitation will propagate until all the oscillators representing the same object are activated. Thus the underlying dynamics of LEGION rapidly achieves both synchronization by local cooperation through excitatory coupling and desynchronization by global competition via the global inhibitor. For rigorous analysis, see Terman and Wang [11] and Wang and Terman [14], [15].

C. Weight Adaptation

Given LEGION dynamics, to extract desired features, we need to form local connections $W_{ij;kl}$ in (2) based on the input image. In LEGION networks, effective couplings in a very local neighborhood, such as the eight nearest neighborhood, are used. Without introducing assumptions about the desired features, $W_{ij;kl}$ in general can be formed based on the intensity values at the corresponding pixels (i, j) and (k, l) in the input image. However, due to variations and noise in real images, individual pixel values are not reliable, and the resulting connections would be noisy and lead to undesirable results.

To overcome this problem, we use a weight adaptation method for noise removal and feature preservation [2]. For each oscillator in the network, two kinds of connections, namely, *fixed* and *dynamic* connections, are introduced. For oscillator (i, j), the fixed connectivity specifies a group of neighboring oscillators that affect the oscillator, and the associated neighborhood is called *lateral* neighborhood $N_l(i, j)$. On the other hand, the dynamic connectivity encodes the transient relationship between two oscillators in a local neighborhood during weight adaption and is initialized based on corresponding pixel values, and the associated neighborhood is called *local* neighborhood $N(i, j)$. To achieve accurate boundary localization, in this communication, $N(i, j)$ is defined as the eight nearest neighborhood of (i, j). Fixed connection weights are established based on the input image, while dynamic connection weights adapt themselves for noise removal and feature preservation, resulting in interactions between two scales. Intuitively, dynamic weights between two oscillators should be adapted so that the absolute dynamic weight becomes small if the corresponding pixels are in a homogeneous region, while the weight should remain relatively large if the corresponding pixels cross a boundary between two homogeneous regions. Based on the observation that most of the discontinuities in the lateral neighborhood $N_l(i, j)$ correspond to significant features, such discontinuities should remain unchanged and be used to control the speed of weight adaptation for preserving features. Such discontinuities in the lateral neighborhood are called *lateral discontinuities* [2]. Furthermore, because proximity is a major grouping principle, *local discontinuities* incorporate changes of attributes among local oscillators. The lateral neighborhood provides a more reliable statistical context, by which the weight adaptation algorithm is governed. The local neighborhood utilizes the statistical context and local geometrical constraints to adaptively change the local connections. These two discontinuity measures are jointly used in weight adaptation.

This method can be viewed as an efficient way of integrating information from multiple scales. However, it is different from multiscale approaches [4]. Instead of applying the same operators on different scales, in lateral neighborhoods, statistical information is derived and used mainly to guide local weight adaptation. In local windows, geometrical constraints are enforced through local coupling, preserving boundaries precisely. The weight adaptation scheme is closely related to nonlinear smoothing algorithms [6]. It preserves significant discontinuities, while adaptively smoothing variations caused by noise. Compared to existing nonlinear smoothing methods, the weight adaptation method offers several distinct advantages [2]. First, it is insensitive to termination conditions, while many nonlinear methods critically depend on the number of iterations. Second, it is computationally fast. Third, by integrating information from different scales, this method generates better results. Quantitative comparisons with other methods, including various smoothing algorithms, are provided in [2].

D. Automated Leader Selection

Both LEGION networks and weight adaptation methods are generic approaches, where no assumption about the features being extracted is made. To extract desired features from remote sensing images, we need to specify relevant features. One way is to use certain parametric forms based on assumptions and heuristics about the properties of features. However, for map revision and other remote sensing applications, images may be acquired under different conditions and even through different sources such as DOQQ images. These factors make it very difficult to model the features using parametric forms. A more feasible way is to specify the desired features using positive and negative examples. Here we use a multilayer perceptron to learn the parameters systematically through user-specified examples.

To apply a multilayer perceptron, a number of design choices must be made. If we present the pixels in the training examples directly to the network, we observe that many training examples are necessary to achieve good results. Due to the potential conflicting conditions, the network often does not converge. To achieve rotational invariance and reduce the necessary number of training samples, we extract several local attributes from training windows as input to the network instead of presenting the training windows directly to the network. More specifically, we use the average value, minimum, maximum, and variance from training samples, and a three-layer (4-3-1) perceptron. These values are normalized to improve training and classification results.

[1]This interpretation is different from a previous one used in [11], [14], [15]. After algebraic manipulations, the equations can be re-written in terms of the previous, more conventional interpretation.

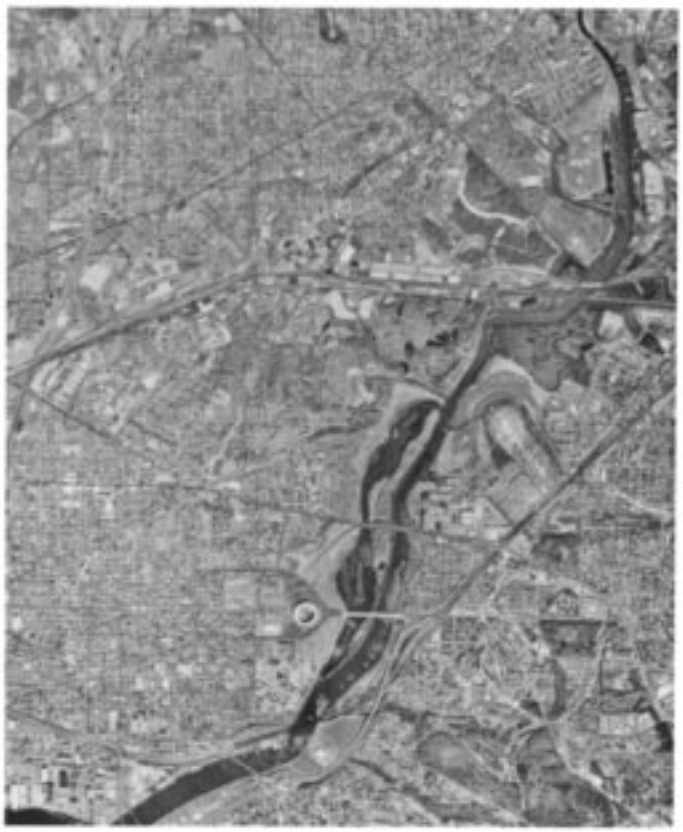

Fig. 1. DOQQ image with 6204 × 7676 pixels of the Washington East, DC/MD area. The Kenil Worth Aquatic Garden is located below the river in the upper right quadrant.

Fig. 2. Extracted hydrographic regions from the DOQQ image shown in Fig. 1. Hydrographic regions are marked as white and superimposed on the original image to show the accuracy of the extracted result. Here, $W_z = 0.15$ and $\theta_p = 4000$. It takes about 100 min on an HP workstation to generate this result.

To further reduce the number of necessary training samples and deal with variations within features being extracted, the multilayer perceptron is applied for leader selection only. In other words, instead of classifying all the pixels directly, we train the network to find pixels that are within large regions to be extracted. The accurate boundaries are then derived using a LEGION network with weight adaptation. As demonstrated in the next section, a small number of training samples are sufficient for very large images with significant variations. In contrast, some existing methods such as [9] often divide the entire data into training and test sets with approximately the same size in order to achieve good performance, ending up using many more training samples.

III. Experimental Results

We have applied the proposed method to extract hydrographic regions from DOQQ images. Given an input image, we construct a two-dimensional (2-D) LEGION network, where each pixel corresponds to an oscillator. A three-layer perceptron is used to determine the leaders in the LEGION network. Oscillators in a major region develop high potentials and thus are oscillating. In this communication, a region is considered to be major if its size is larger than a threshold θ_p. The dynamic connection $W_{ij;kl}$ between oscillator (i, j) and (k, l) is established based on the weight adaptation method. Extracted regions correspond to all the oscillating oscillators.

Fig. 1 shows a DOQQ image from the Washington East, DC/MD area. The training samples are chosen manually to represent typical samples from hydrographic and nonhydrographic regions. The trained network is then applied to classify the entire DOQQ image. While the pixels in central and major river regions are correctly classified, the river boundaries are rough. Also, there are pixels that are misclassified as hydrographic seed points even though they do not belong to any hydrographic regions. The false target rate is 1.97%. Here, the false target rate is the ratio of the number of nonhydrographic pixels that are misclassified to the total number of true hydrographic pixels. Similarly, the false nontarget rate is the ratio of the number of hydrographic pixels that are misclassified to the total number of true hydrographic pixels. The ground truth is generated by manual seed selection based on a 1 : 24 000 topographic map from the United States Geological Survey, Boulder, CO. We then apply a LEGION network with weight adaptation. Leaders in LEGION are determined with $\theta_p = 4000$. Because noisy seed points cannot develop high potentials, no hydrographic regions are extracted around those pixels. Extracted hydrographic regions are shown in Fig. 2. Both the false target and false nontarget rates are reduced dramatically. The false target rate is reduced to 0.75%. Also, the hydrographic region boundaries are localized much more accurately, and thus, the false nontarget rate is reduced. Mainly because the Kenil Worth Aquatic Garden (see Fig. 1), where pixels are statistically very similar to soil land, is not extracted, the false nontarget rate of the proposed method still stands at 11.70%. If we assume that leaders are correctly detected in the area, the proposed method can correctly extract the aquatic region with high accuracy. All major hydrographic regions are extracted with accurate boundaries and cartographic features, such as bridges and islands, are preserved well, which are critically important for deriving accurate spatial information. The major river, Anacostia River, is extracted correctly, and several roads crossing the river are preserved.

To demonstrate the effectiveness of our method in preserving important cartographic features, Fig. 3(a) shows an area around the Kingman

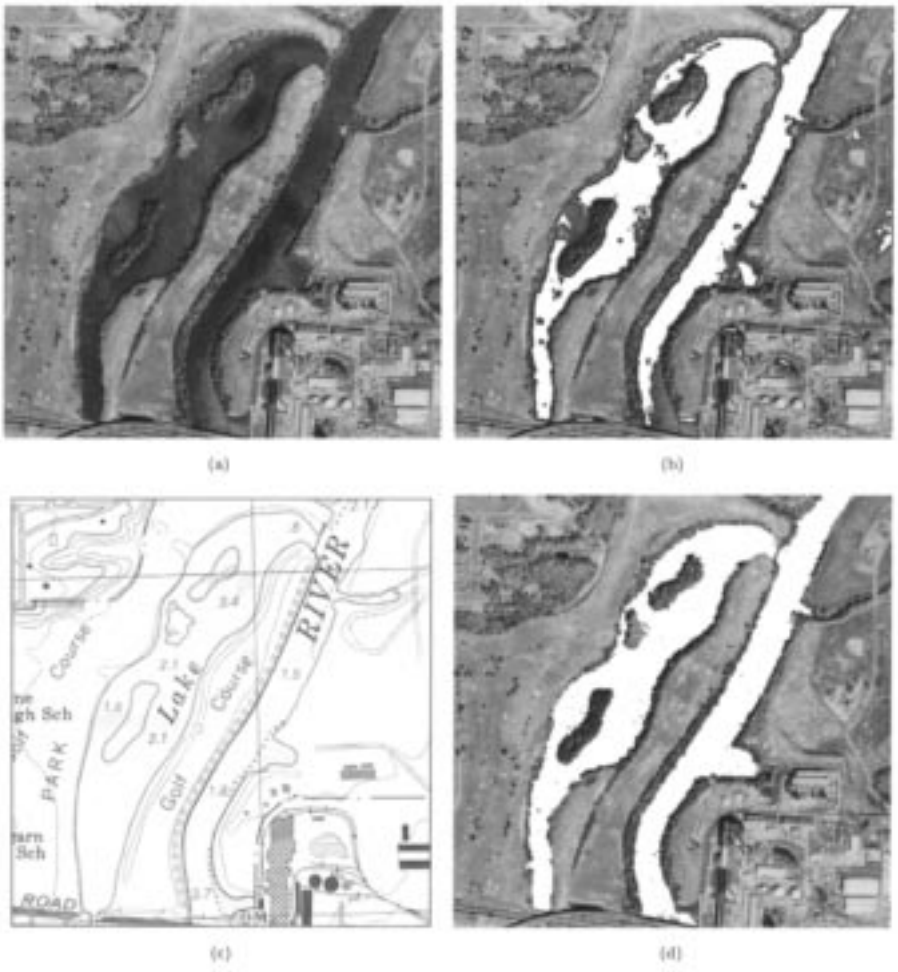

Fig. 3. Extraction result for an image patch from the Washington East DC/MD area: (a) Input image. (b) Seed points from the neural network. (c) Topographic map of the area. Here, the map is scanned from the hardcopy and not wrapped with respect to the image. (d) Extracted result from the proposed method. Extracted regions are represented by white and superimposed on the original image.

Lake. Within this image, intensity values and local attributes change considerably. Fig. 3(b) shows the classification result using the multilayer perceptron, Fig. 3(c) shows the corresponding part of the USGS 1 : 24 000 topographic map, and Fig. 3(d) shows our result. The boundaries of small islands are localized accurately even though they are covered by forests. In weight adaptation, the information from the lateral and local windows is jointly used when variances in a local neighborhood are large, resulting in robust feature preservation and noise removal. Similarly, the forests along the river banks are preserved well. A bridge that connects the lake and the river is also preserved. As shown in Fig. 3(a), the bridge is spatially small and it would be very difficult for nonlinear smoothing algorithms to preserve this important cartographic feature.

By comparing Fig. 3(a) and (c), one can see that hydrographic regions have changed from the map. Note, for example, the lower part of the left branch. This geographical change illustrates the constant nature of such changes and the need for frequent map revision. With precise region boundaries produced by our method, our system is suited for map revision purposes. For example, the lake has shrunk in size, and such shrinkage is well captured by our algorithm [see Fig. 3(d)]. This suggests that our method can be used for monitoring changes of hydrographic features.

To summarize, the results generated for DOQQ images are comparable with the hydrographic regions shown in the United States Geological Survey 1 : 24 000 topographic maps. In certain cases, our results reflect better the current status of geographical areas than the corresponding topographic maps.

IV. Conclusion

In this communication, we have presented a computational framework for extracting geographic features from remote sensing images, and have applied our system to DOQQ images with good results. Compared with traditional map-making methods based on aerial photogrammetry, our method is computationally efficient. We believe that this kind of technology is effective for improving map revision and other remote sensing applications. Furthermore, because remotely sensed images can be captured more readily with high resolutions, efficient methods like the one proposed here should be very useful for extracting up-to-date and accurate geographic information.

Acknowledgment

The authors would like to thank the reviewers for their valuable comments and suggestions.

References

[1] J. A. Benediktsson and J. R. Sveinsson, "Feature extraction for multisource data classification with artificial neural networks," *Int. J. Remote Sensing*, vol. 18, no. 4, pp. 727–740, 1997.

[2] K. Chen, D. L. Wang, and X. Liu, "Weight adaptation and oscillatory correlation for image segmentation," *IEEE Trans. Neural Networks*, vol. 11, pp. 1106–1123, Sept. 2000.
[3] S. Gopal and C. Woodcock, "Remote sensing of forest change using artificial neural networks," *IEEE Trans. Geosci. Remote Sensing*, vol. 34, pp. 398–404, Mar. 1996.
[4] T. Lindeberg and B. M. ter Haar Romeny, "Linear scale-space," in *Geometry-Driven Diffusion in Computer Vision*, B. M. ter Haar Romeny, Ed. Dordrecht, The Netherlands: Kluwer, 1994, pp. 1–41.
[5] X. Liu and D. L. Wang, "Range image segmentation using an oscillatory network," *IEEE Trans. Neural Networks*, vol. 10, pp. 564–573, May 1999.
[6] P. Perona and J. Malik, "Scale-space and edge detection using anisotropic diffusion," *IEEE Trans. Pattern Anal. Machine Intell.*, vol. 12, pp. 629–639, 1990.
[7] S. Sarkar and K. L. Boyer, "On optimal infinite impulse response edge detection filters," *IEEE Trans. Pattern Anal. Machine Intell.*, vol. 13, pp. 1154–1171, 1991.
[8] N. Shareef, D. L. Wang, and R. Yagel, "Segmentation of medical images using LEGION," *IEEE Trans. Med. Imag.*, vol. 18, pp. 74–91, Jan. 1999.
[9] A. H. S. Solberg, T. Taxt, and A. K. Jain, "A Markov random field model for classification of multisource satellite imagery," *IEEE Trans. Geosci. Remote Sensing*, vol. 34, pp. 100–113, Jan. 1996.
[10] C. Sun, C. M. U. Neale, J. J. McDonnell, and H. D. Cheng, "Monitoring land-surface snow conditions from SSM/I data using an artificial neural network classifier," *IEEE Trans. Geosci. Remote Sensing*, vol. 35, pp. 801–809, July 1997.
[11] D. Terman and D. L. Wang, "Global competition and local cooperation in a network of neural oscillators," *Phys. D*, vol. 81, pp. 148–176, 1995.
[12] D. Tsintikidis, J. L. Haferman, E. N. Anagnostou, W. F. Krajewski, and T. F. Smith, "A neural network approach to estimating rainfall from spaceborne microwave data," *IEEE Trans. Geosci. Remote Sensing*, vol. 35, pp. 1079–1093, Sept. 1997.
[13] C. von der Malsburg, "The correlation theory of brain function," Max-Planck-Institut for Biophysical Chemistry, Göttingen, Germany, Int. Rep. 81-2, 1981.
[14] D. L. Wang and D. Terman, "Image segmentation based on oscillatory correlation," *Neural Comput.*, vol. 9, pp. 805–836, 1997.
[15] ——, "Image segmentation based on oscillatory correlation," *Neural Comput.*, vol. 9, pp. 1623–1626, 1997.

New Sampling Method for the Improvement of the Image Reconstruction Algorithm for the Rotating Object

Gum-Sil Kang and Yong-Hoon Kim

***Abstract*—The proposed method is devised to reconstruct a focused radar image for a wide observation angle without an interpolation, and therefore, it improves the image quality and reduces the processing time. To evaluate the performance, it is compared with the conventional sampling method through simulation and experimental results. In the case of the proposed method, the computation time is improved more than 33% for the image size of 1024 × 1024 pixels.**

***Index Terms*—Image reconstruction, inverse synthetic aperture radar (ISAR), sampling method.**

I. Introduction

A high resolution inverse synthetic aperture radar (ISAR) imaging technique for a controllable rotating target has been used in various application areas, including modeling and analysis of radar targets [1]. Also, it has been adopted as a diagnostic method to support the medical and physical sciences and used to develop the target detection, recognition, and classification techniques [2], [3]. In stepped frequency ISAR, generally the reflected radar signal is sampled on the polar coordinates of frequency and observation angle [4]. This method will be referred to as the conventional sampling method in this paper. For a small observation angle, a high resolution image can be achieved with short processing time using the unfocused reconstruction algorithm because the received data can be modeled by samples of the Fourier transform on rectangular coordinates [5], but if the angle range is not very small, the unfocused image is degraded by the blur effect. Also, the matrix pencil method was proposed to achieve much higher resolution than the conventional FFT method in case of small data aperture [6], but it is not evaluated on the performance for a wide angle. The blur effect can be removed by the reformatting of received data on rectangular lattice using the interpolation in the focused image. However, the additional interpolation process causes a longer processing time than the unfocused algorithm and the image degradation due to artifacts. In this paper, a new sampling method is proposed to obtain a focused image for a wide observation angle without an interpolation process. The simulation and experiment results show that this method has a lower complexity and shorter processing time than the conventional method, and the image degradation due to artifacts has been reduced remarkably.

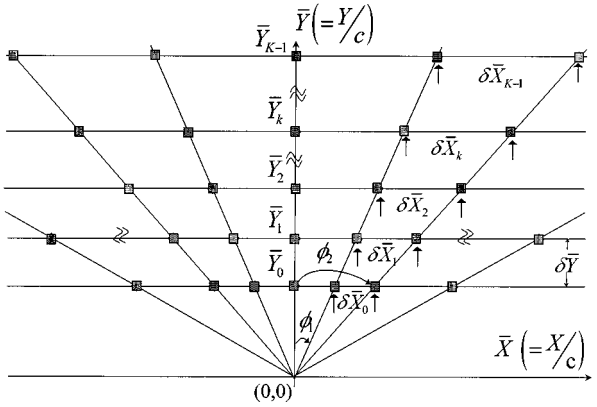

Fig. 1. Measurement coordinate for new sampling method.

II. New Sampling Method for Image Reconstruction of Rotating Targets

The new sampling method is devised to measure the reflected radar signal from targets directly on a rectangular raster by use of controlled frequency and rotation angle. Fig. 1 shows the sampling coordinates for the new sampling scheme. The sampling positions are determined by the observation angle ϕ and the frequency f of radar waveforms through (1). The reflected signal is sampled with interval $\delta\overline{X}_k$ along the $\overline{X}$ axis for any fixed point $\overline{Y}_k$ and also with interval $\delta\overline{Y}$ along the $\overline{Y}$ axis. Where $\overline{X}(=X/c)$, $\overline{Y}_k(=Y/c)$, $\delta\overline{X}_k(=\delta X_k/c)$, and $\delta\overline{Y}(=\delta Y/c)$ are normalized values of X, Y, δX_k, δY by the light velocity c. The start frequency, the step frequency, and the interval of observation angle should be controlled during the measurement of the reflected signal. To determine the start frequency and the step frequency at a given observation angle, the initial value $\overline{Y}_0$, and the interval of measurement $\delta\overline{Y}$ should be selected according to (2) and (3), respectively, where f_{s_0} is the start frequency when the angle of rotation ϕ is equal to zero. The measurement interval $\delta\overline{Y}$ should be

Manuscript received June 29, 1999; revised December 27, 1999. This work was supported in part by BK21 (Brain Korea), and the Advanced Environmental Monitoring Research Center, Kwangju Institute of Science and Technology, KOREA Science and Engineering Foundation (KOSEF), Kwangju, Korea.

The authors are with the Department of Mechatronics, Kwangju Institute of Science and Technology, Kwangju 500-712, Korea (e-mail: kgs@geguri.kjist.ac.kr; jhkim@kjist.qc.kr).

Publisher Item Identifier S 0196-2892(01)00476-4.